Global Journal of Chemistry, Biology and Physics
Volume.8, Number 2;April-June, 2023;
ISSN: 2836-9572| Impact Factor: 7.49
https://zapjournals.com/Journals/index.php/gjcbp
Published By: Zendo Academic Publishing

ANTIOXIDANT AND THERMAL PROPERTIES OF ZN(II), FE(II), AND MN(II) COMPLEXES WITH THIOPHENE-CARBOXYLATE LIGAND: SYNTHESIS AND CHARACTERIZATION"

Mehmet Can Aydın[1], Esra Nur Kaya[2], Burak Emre Yılmaz[3]

Article Info

Keywords: Schiff-base ligands, transition metal complexes, biological activity, catalysis, heterocyclic molecules.

Abstract

Schiff-base ligands featuring heterocyclic moieties and heteroatoms such as N, O, and S have garnered significant attention in the realm of chemistry and biology due to their diverse biological activities and their remarkable interactions with transition metal ions. These complexes have been identified as effective and stereo-specific catalysts for a range of chemical reactions, including oxidation, reduction, and hydrolysis, while also exhibiting substantial biological potential. The current review explores the multifaceted applications of Schiff-base complexes derived from both transition and non-transition metals, shedding light on their role as promising materials for various catalytic, sensing, and medicinal applications.

1. Introduction

Schiff-base ligands with heterocyclic molecule and/or containing heteroatoms such as N, O, and S show a broad biological activity and are of special interest because of the variety of ways in which they are interacted to transition metal ions (Ahmed et al., 2013).

The complexes make these compounds effective and stereo specific catalysts for oxidation, reduction and hydrolysis and they show biological activity, and other transformations of organic and inorganic chemistry (Ramesh & Sivagamasundari, 2003). This class of complexes obtained from transition and non-transition metals has emerged as very promising materials for their use as efficient catalysts (Padma Priya et al., 2009), biological sensors (Yu et al., 2008), antibacterial, antifungal, antiviral, antioxidant, herbicidal and also as anticancer agents (Kabeer et al., 2001; El-Masry et al., 2000; Manjunatha et al., 2011; Kiran et al., 2006; Ilhan et al., 2014). In this respect, the formation of metal complexes plays an important role to enhance their biological activity. Studies have also shown that the azomethine nitrogen which has a lone pair of electrons in a sp^2 hybridised orbital has considerable biological importance (Rabbi et al., 1998).

In view of biological importance of Schiff base derived from the condensation of ethyl 2-amino-6-methyl-4,5,6,7-tetrahydrobenzo[b]thiophene-3-carboxylate with salicylaldehyde, its applications in various fields, in the present

---

[1] Department of Chemistry, Faculty of Arts and Sciences, Muş Alparslan University, 49250 Muş, Turkey[1,2,*3]

investigation it is thought to synthesize the metal complexes with transition metal ions such as Zn(II), Fe(II) and Mn(II).

Based on the mentioned properties of Schiff bases and its complexes, in our present study we report their synthesis, spectroscopic characterization. Also, we investigated antioxidant properties of ligand and its complexes by reducing antioxidant power assay, DPPH·radical scavenging, $ABTS^{\bullet+}$ radical scavenging, ferric thiocyanate method, separately.

2. Experimental

2.1. Materials and Measurements

All commercially available chemicals are of reagent grade and were used as received without further purification. They included salicylaldehyde (Merck), $CaCl_2$ (Merck). $FeCl_2.H_2O$ (Sigma), $ZnCl_2.2H_2O$ (Sigma) and $MnCl_2.4H_2O$ (Sigma) were used. Also, chemicals for antioxidant activities such as ABTS (2,2-azinobis 3ethylbenzthiazoline-6-sulfonic acid), DPPH (1,1-diphenyl-2-picryl-hydrazyl), ascorbic acid (99%), polyoxyethylene sorbitan monolaurate (Tween-20), linoleic acid, BHA (Butylated hydroxyanisole), BHT (Butylated hydroxytoluene) and trichloroacetic acid (TCA) were obtained from Sigma (Sigma-Aldrich GmbH, Sternheim, Germany).

Organic solvents used included absolute ethanol, methanol, diethyl ether, chloroform, glacial acetic acid and dimethylformamide (DMF). These solvents were provided spectroscopically pure from Merck. Elemental analyses of C, H, and N were taken on a Leco CHNS-O model 932 elemental analyzer. IR spectra were recorded Perkin Elmer Precisely Spectrum One spectrometer on KBr discs in the wave number range of 4000-400 cm^{-1}. ^{1}H-NMR and ^{13}C-NMR spectra were recorded using a model Bruker GmbH DPX-400 MHz FT spectrometer. Electronic spectral studies were conducted on a Shimadzu model UV-1800 Spectrophotometer in the wavelength 1100-200 nm. Magnetic susceptibilities measurements were performed using the standard Gouy tube technique using $Hg[Co(SCN)_4]$ as a calibrate. The molar conductance of solid complexes in DMF was measured using Siemens WPA CM 35 conductometer. Thermal analyzers (TGA and DTA) were carried out in nitrogen atmosphere with a heating rate of 10 °C/min. using Shimadzu DTG-60 AH (Shimadzu DSC 60 A) thermal analyzers. LC/MS-API-ES mass spectra were recorded using an AGILENT model 1100 MSD mass spectrophotometer.

2.2. Synthesis of Ligand

An ethanol solution (20 mL) containing ethyl 2-amino-6-methyl-4,5,6,7tetrahydrobenzo[b]thiophene-3-carboxylate (0.80 g, 0.003 mol) was added drop wise to an ethanol solution (15 mL) of salicylaldehyde (1.03 g, 0.003 mol) with five drops of glacial acetic acid as catalyst. After refluxed for 2 h, the resultant solution was filtered. Proposed structure of ligand and its complexes were showed in Figures 1-3.

Characterization of ligand: [Yield: 84%] m.p.: 96-98 $^{\circ}$C; FW: 343.44 g/mol; ^{1}H NMR ($CDCl_3$, 400 MHz) δ H20: 10.71 (s, 1H), H19: 8.77 (s, 1H), H13-H18: 7.68-6.95 (m, 4H), H10:4.30 (q, 2H), H3: 2.85 (d, 2H), H6: 2.64 (t, 2H), H2: 2.06 (m, 1H), H10H11:1.87-1.04 (m, 6H), H1: 1.74 (q, 2H); ^{13}C NMR (DMSO-d_6, 400 MHz) δ 14.86 ($CH_{3\text{-}C10}$), 21.75 ($CH_{3\text{-}C11}$), 26.72 ($CH_{2\text{-}C6}$), 29.41 ($CH_{2\text{-}C3}$), 31.00 ($CH_{\text{-}C2}$), 32.50 ($CH_{2\text{-}C1}$), 59.10 ($CH_{2\text{-}C10}$), 131.41, 126.52, 131.41, 115.86 ($CH_{\text{-}C13\text{-}15,18}$), 163.43, 115.49 ($C_{\text{-}C16\text{-}17}$), 163.43 ($CH{=}N_{\text{-}C19}$), 148.62, 131.41 ($C\text{-}S\text{-}C_{\text{-}C4\text{-}9}$), 153.49 ($C{=}O_{\text{-}C10}$); IR (KBr, cm^{-1}) ν: 3367 (OH), 3196-3054 (Ar-CH), 2924 (Alip.-CH), 1698 (C=O), 1620 (CH=N), 15681557 (Ar-C=C), 1255 (C-O), 751 (C-S-C); Anal. Calcd. for $C_{19}H_{21}NSO_3$: C, 66.45; H, 6.16; N, 4.48; S, 9.34. Found: C, 66.33; H, 6.33; N, 4.14; S, 9.41. MS [ESI+]: *m/z* 345.50 $[L+2H]^{2+}$. Color: Yellow.

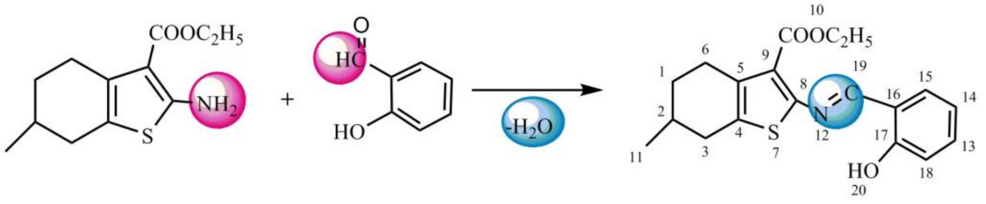

Fig. 1: Scheme synthesis of ligand

2.3. Synthesis of Metal Complexes

A hot ethanol solution of $ZnCl_2 \cdot 2H_2O$ metal salt (0.002 mol, 0.34 g) was added to an ethanol solution of the (*E*)-ethyl-2-(2-hydroxy-3-methoxybenzylideneamino)-6-methyl-4,5,6-tetrahydrobenzo[b]thiophene-3carboxylate ligand (0.001 mol, 0.34 g), heated under reflux for 4 h. The solid complex precipitate was filtered off and washed thoroughly with ethanol and diethyl ether and dried over anhydrous $CaCl_2$ under vacuum.

$[Zn_2LCl_3(H_2O)_5] \cdot 6H_2O$: [Yield: 53%] m.p.: 256-259 °C; FW: 777.53 g/mol; IR (KBr, cm^{-1}) ν: 3522, 3390 (OH), 3120-3060 (Ar-CH), 2951, 2929 (Alip.-CH), 1672 (C=O), 1607 (CH=N), 1573-1540 (Ar-C=C), 1232 (C-O), 766 (C-S-C), 569, 546 (M-O), 472 (M-N), 462 (M-S); Anal. Calcd. for $C_{19}H_{42}NSO_{14}Zn_2Cl_3$: C, 29.32; H, 5.40; N, 1.80; S, 4.12. Found: C, 29.33; H, 5.45; N, 1.86; S, 4.18. MS [ESI+]: *m/z* 775.14 (calcd.), 775.80 (found) $[M-2H]^{2-}$. Color: Brown.

An amount of (0.002 mol, 0.68 g) the ligand was dissolved in 20 mL ethanol, and a solution of $FeCl_2 \cdot H_2O$ (0.001 mol, 0.14 g) in 20 mL ethanol was added drop wise with continuous stirring; the dark product was appeared after one night. The mixture was stirred for 4 h. The resulting precipitates were filtered and washed with ethanol and dried over anhydrous $CaCl_2$ under vacuum.

$[FeL_2] \cdot H_2O$: [Yield: 63%] m.p.: 211 °C; FW: 758.88 g/mol; IR (KBr, cm^{-1}) ν: $3400_{(broad)}$ (OH), 3180, 3062 (Ar-CH), 2921 (Alip.-CH), 1697 (C=O), 1598 (CH=N), 1568-1530 (Ar-C=C), 1223 (C-O), 761 (C-S-C), 540, 521 (M-O), 495, 478 (M-N), 464 (M-S); Anal. Calcd. for $C_{38}H_{42}N_2S_2O_7Fe$: C, 60.09; H, 5.53; N, 2.65; S, 8.43. Found: C, 60.08; H, 5.50; N, 2.70; S, 8.47. MS [ESI+]: *m/z* 729.88 (calcd.), 729.70 (found) $[M-C_2H_5]^-$. μ_{eff} (B.M.): 4.92, Color: Black.

The $MnCl_2 \cdot 4H_2O$ (0.002 mol, 0.39 g) in 30 mL of ethanol was added to a hot solution of the ligand (0.002 mol 0.68 g) in 20 mL of ethanol. The reaction mixture was heated under reflux for 3 h and then the volume was reduced to half of the initial volume under reduced pressure. The separated precipitate was filtered off, washed with water, ethanol and finally with diethyl ether and then dried in air at room temperature.

$[MnLCl(H_2O)_2] \cdot 2H_2O$: [Yield: 58%] m.p.: 222 °C; FW: 504.39 g/mol; IR (KBr, cm^{-1}) ν: 3493, 3400 (OH), 3187, 3062 (Ar-CH), 2924, 2861 (Alip.-CH), 1698 υ(C=O), 1598 (CH=N), 1552 (Ar-C=C), 1234, 1216 (C-O), 779 (C-S-C), 540 (M-O), 474 (MN), 460 (M-S); Anal. Calcd. for $C_{19}H_{28}NSO_7MnCl$: C, 45.15; H, 5.55; N, 2.77; S, 6.33. Found: C, 45.55; H, 5.32; N, 2.80; S, 6.30. MS [ESI+]: *m/z* 502.45 (calcd.), 502.30 (found) $[M-2H]^{2-}$. μ_{eff} (B.M.): 5.80, Color: Dirty brownish.

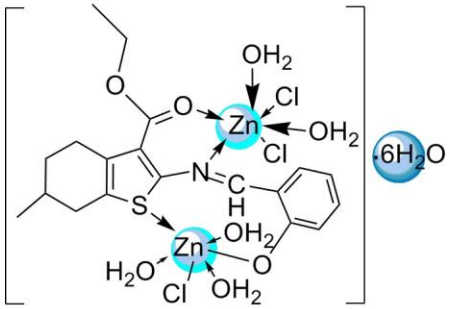

Fig. 2: Structure of $[Zn_2LCl_3(H_2O)_5]\cdot6H_2O$ complex

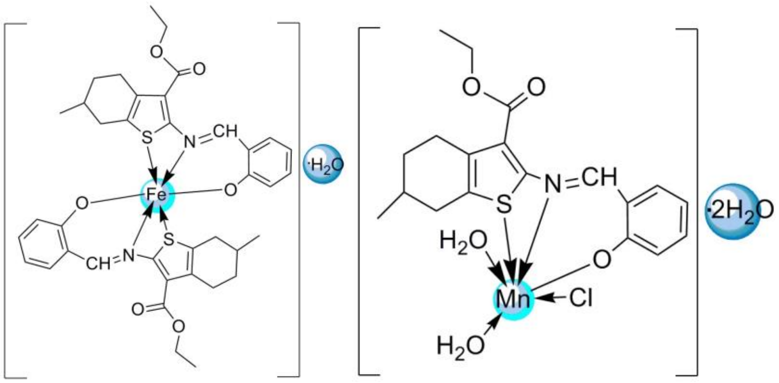

Fig. 3: Structure of $[FeL_2]\cdot H_2O$ and $[MnLCl(H_2O)_2]\cdot2H_2O$ complexes

2.4. DPPH• Scavenging Activity

The DPPH free radical scavenging activity of ligand and its complexes were evaluated by the method described in the literature (Koksal et al., 2009). Briefly, different concentrations (10-30 µg/mL) of samples and standard antioxidants (BHA, BHT and ascorbic acid) were prepared and diluted to 3 mL with ethanol. Then, 1 mL of ethanolic DPPH solution (0.1 mM) was added to the samples. These samples were vortexed and incubated in the dark at 30 ºC for 30 min. The absorbance was measured at 517 nm against blank samples. A decrease in absorbance indicates DPPH free radical scavenging activity.

2.5. $ABTS^{\bullet+}$ Scavenging Activity

The $ABTS^{\bullet+}$ radical scavenging activity of ligand and its complexes were evaluated according to the method described in the literature (Bursal & Gulcin, 2011). $ABTS^{\bullet+}$ is blue-green in color with a characteristic absorbance at 734 nm. $ABTS^{\bullet+}$ cation radical was produced by reacting ABTS (2 mM) in H_2O and potassium persulphate (2.45 mM) at room temperature for 12 h. The $ABTS^{\bullet+}$ solution was diluted with phosphate buffer (0.1 M, pH 7.4) to achieve an absorbance of 0.750 ± 0.025 at 734 nm. Then, 1 mL of $ABTS^{\bullet+}$ solution was added to 3 mL of extract solution in methanol at different concentrations (10-30 µg/mL) of samples and standard antioxidants (BHA, BHT and ascorbic acid). These samples were vortexed and incubated in the dark for 30 min. After 30 min, the absorbance at 734 nm was measured for each concentration relative to a blank. Decreased absorbance of the samples indicates $ABTS^{\bullet+}$ cation radical scavenging activity.

2.6. Ferric Reducing Antioxidant Power (FRAP)

The reducing power of ligand and its complexes were measured according to the method described in the literature (Bursal & Koksal, 2011). According to this method, the reduction of Fe^{3+} to Fe^{2+} is determined by measuring the absorbance of Perl's Prussian blue complex. Briefly, different concentrations (10-30 µg/mL) of samples and standard antioxidants (BHA, BHT and ascorbic acid) in distilled water (0.75 mL) were mixed with 1 mL of sodium phosphate buffer (0.2 M, pH 6.6) and 1 mL (1%) of potassium ferricyanide [$K_3Fe(CN)_6$]. The mixture was incubated at 50 ºC for 20 min. Then, the reaction mixture was acidified with 1 mL of trichloroacetic acid (10%). Finally, 0.25 mL of iron (III) chloride (0.1%) was added to this solution.

The absorbance of the mixture at 700 nm was measured. A decrease in absorbance indicates increased ferric reducing antioxidant power.

2.7. Total Antioxidant Activity Determination

The ferric thiocyanate method was used to evaluate the effect of ligand and its metal complexes on the prevention of peroxidation of linoleic acid emulsion, as described previously in the literature (Gulcin et al., 2010). For preparing stock solutions, 10 mg of samples and standard antioxidants (BHA, BHT and ascorbic acid) were dissolved in 10 mL distilled water, separately. 20 µg/mL of samples were prepared by diluting the stock solution in 2.5 mL of sodium phosphate buffer (0.04 M, pH 7.0) and these were added to 2.5 mL of linoleic acid emulsion in sodium phosphate buffer (0.04 M, pH 7.0). The linoleic acid emulsion was prepared by homogenizing 15.5 µL of linoleic acid, 17.5 mg of Tween-20 as emulsifier, and 5 mL phosphate buffer (pH 7.0).

The control was composed of 2.5 mL of linoleic acid emulsion and 2.5 mL 0.04 M sodium phosphate buffer (pH 7.0). The reaction mixtures (5 mL) were incubated at 37 ºC in polyethylene flasks. The peroxide levels were determined by reading the absorbance at 500 nm in a spectrophotometer (Shimadzu, UV-1800 UVVis Spectrophotometer, Japan) after reactions with $FeCl_2$ and thiocyanate at intervals during incubation. The peroxides formed during linoleic acid peroxidation oxidize Fe^{2+} to Fe^{3+}, and Fe^{3+} forms a complex with thiocyanate that has a maximum absorbance at 500 nm. The assay steps were repeated every 12 hour until the maximum was reached. The percentage of inhibition was calculated at this maximum point. (A_{sample}: Absorbance of sample at 500 nm, $A_{control}$: Absorbance of control at 500 nm)

$$\text{Inhibition of lipid peroxidation}\ (\%) = \left(1 - \frac{A_{sample}}{A_{control}}\right) \times 100$$

3. Results and Discussion

3.1. Spectral Studies

The tentative assignments of the significant IR spectral bands of the free ligand and its complexes are presented in experimental section.

The complexes are found to be air stable. The ligand is soluble in common organic solvents and all the complexes are freely soluble in $CHCl_3$, DMF and DMSO.

A band characteristic of υ(OH) of phenol group is observed at 3367 cm^{-1} in the spectrum of ligand. The disappearance of this vibration band associated with the stretching OH of the phenolic group in all the complexes reveals the loss of phenolic proton on complexation, forming metal-oxygen bond (Al-Juburi, 2012). The Zn(II) and Mn(II) complexes show a broad band in the range of 3522-3390 cm^{-1} followed by another band at 817-815 cm^{-1}, which is due to characteristic of υ(OH) of coordinated water (Jezowska-Trzebiatowska et al., 1988). Sharp bands observed in the spectrum of the free ligand at approximately 1620 cm^{-1} are assigned to υ(CH=N) (Ali et al., 1995). In the metal complexes this absorption was shifted to lower frequencies indicating coordination of the azomethine nitrogen to the central metal atoms. The absorption band appearing in the ligand spectra at 751 cm^{-1}due to the υ(C-S-C) is shifted to lower or higher wave numbers by 10-28 cm^{-1} in the complexes spectra, suggesting coordination through the sulfur atom. On the other hand, the ligand band at 1698 cm1 which assigned to υ(C=O) of the ester carbonyl appears, almost at the same position, in the spectra of Fe(II) and Mn(II) complexes. The new bands in the region 569-521 cm^{-1} 495-472 cm^{-1} and 464-460 cm^{-1} in the spectra of the complexes are assigned to stretching frequencies of υ(M-O), υ(M-N) and υ(M-S) bonds respectively (Etaiw et al., 1995; Moustafa, 1997). This indicates that phenolate O, azomethine N atoms and thiophene S are involved in coordination (Jouad et al., 2001).

The ^{1}H and ^{13}C-NMR spectra of the ligand were recorded using $CDCl_3$ as the solvent and obtained data are given in experimental section. In the ^{1}H-NMR spectra of the ligand, the broad signals in the 10.71 ppm range can be attributed to the proton of the phenolic OH group. The signal belonging to the OH proton disappears in D_2O solution. The signal of the hydrogen atoms of the azomethine group was seen at 8.77 ppm. The multiples of the hydrogen atoms of the aromatic rings were determined in the 7.68-6.95 ppm range. The Zn(II) complex is diamagnetic and NMR active. The absence of the OH proton peak and upfield shift (δ: 0.8 ppm) of the CH=N proton peak (δ: 8.88 ppm) in complex Zn(II), with respect to the corresponding free ligand, indicate the complexation with Zn(II). The aromatic protons (H13–H18) of the complex Zn(II) were detected as multiplet in the aromatic region 7.85-7.32 ppm.

In the ^{13}C-NMR spectra of the ligand, the signal at 163.43 ppm can be assigned to the azomethine carbon atom. Aromatic ring carbon atoms of the ligand were determined in the 115.00-163.00 ppm range.

3.2. Molar Conductance

The complexes are non-electrolytes as shown by their molar conductivity (Λ_M) measurements in DMF (0.001 M), which are in the range for Zn(II), Fe(II) and Mn(II) complexes at 17.54, 10.40 and 15.62 $\Omega^{-1}cm^{2}mol^{-1}$, respectively.

3.3. Magnetic Moment Measurements and Electronic Spectra

The magnetic susceptibility results of transition metal complexes give an indication of the geometry of the ligands around the central metal ion. The Zn(II) complex in the present study is diamagnetic, Fe(II) and Mn(II) complexes are paramagnetic. The magnetic measurements for Mn(II) and Fe(II) complexes showed magnetic moment values of 4.92 and 5.80 B.M., respectively, suggesting consistency with their octahedral environment.

The UV-Vis spectrum of ligand shows a high intense absorption peak at 321 nm with a shoulder at 267 nm, assigned to $n\rightarrow\pi^*$ and $\pi\rightarrow\pi^*$, respectively (Lever, 1984). These bands are shifted to 278, 288-347 and 275-359 nm, respectively, which can be attributed to the binding of these coordination centers to the central metal ions. The UV–vis spectra of the complexes display bands at 316, 500 and 670 nm which can be attributed to d–d transition within Zn(II), Mn(II) and Fe(II) complexes, respectively.

The electronic transition spectrum of the brown Zn(II) complex shows shoulder band at 316 nm. This band can be attributed to the LMCT transition and it is consistent with octahedral geometry. The Zn(II) complex is found to be diamagnetic as expected for d^{10} configuration.

The Fe(II) complex has a magnetic moment value of 4.92 B.M. which is consistent with high spin octahedral geometry (Lever, 1984; Sharaby, 2005).

The magnetic moment value (5.80 B.M.) observed for Mn(II) complex suggests the presence of five unpaired electrons. A band observed at 500 nm in Mn(II) complex may be assigned to the $^{6}A_{1g}\rightarrow{}^{4}T_{1g}$ (Mohamed, 2001).

3.4. Mass Spectra

The mass spectra of Zn(II), Fe(II) and Mn(II) Schiff-base complexes respectively, have been recorded. All the spectra exhibit parent peaks due to molecular ions (M^+). The proposed molecular formula of these complexes was confirmed by comparing their molecular formula weights with m/z values. The molecular ion (M^+) peaks obtained for various complexes are as follows: m/z = 775 (Zn(II) complex), m/z = 729 (Fe(II) complex), m/z = 502 (Mn(II) complex).

3.5. Thermal Analysis

The weight loss of thermal gravimetric analysis (TGA) for ligand and its complexes was calculated for the different steps and compared with those of theoretically calculated for the suggested formula based on the results of elemental analysis and mass spectra. In the present investigation heating rates were suitably controlled at 10 °C/min under nitrogen atmosphere and the weight loss was measured from the ambient temperature up to ≈ 800 °C. The TGA curve of ligand showed that this ligand decomposed in one step from 100 to 470 °C. This step corresponds to the complete decomposition of ligand as deduced from mass loss calculation (found mass loss = 97.57%, calcd. mass loss = 99.0%).

TGA curve of the $[Zn_2LCl_3(H_2O)_5]\cdot6H_2O$ indicates that the complex is thermally decomposed in three steps in the temperature range from 50 to 600 °C. The first stage of decomposition occurs in the 50-130 °C temperature range corresponding to the loss of uncoordinated water molecules and is accompanied by a weight loss of 13.89%. The second and third stages of decomposition involve the removal of coordinated water molecules and ligand molecules in the 130-600 °C temperature range and were accompanied by weight loss of 63.33%. The total weight loss amounts to 76.90% (calcd 77.73%) leaving two zinc oxide as residues.

TGA curve of the $[FeL_2]\cdot H_2O$ indicates that the complex is thermally stable to 50 °C. Decomposition of the complex started at 50 °C and finished at 600 °C with four stages.

The first stage of decomposition occurs in the 50-170 °C temperature range corresponding to the loss of H_2O molecule and is accompanied by a weight loss of 2.14%. The second stage of decomposition involves the removal of $COOC_2H_5$ molecule in the 170-200 °C temperature range and is accompanied by a weight loss of 10.00%. While the last two stages involve the removal of two ligand molecules in the 200-600 °C temperature range, and are accompanied by weight loss of 81.23% (calcd 80.51%).The total weight loss amounts to 93.37% (calcd 92.50%) leaving iron metal as residues.

TGA curve of the $[MnLCl(H_2O)_2]\cdot2H_2O$ shows three steps of decomposition. The first stage of decomposition occurs in the 50-120 °C temperature range corresponding to the loss of $2H_2O$ molecule and is accompanied by a weight loss of 7.14% (calcd 7.14%). The second stage of decomposition involves the removal of $2H_2O$ and Cl molecules in the 120-300 °C temperature range and is accompanied by a weight loss of 14.29% (calcd 14.27%). While the third stage involve the removal of $C_{19}H_{20}NSO_2$ molecule in the 300-600 °C temperature range and is accompanied by a weight loss of 64.30% (calcd 64.63%). The total weight loss amounts to 85.73% (calcd 86.04%) and manganese oxide were remained as residues.

3.6. Structural Interpretation

Single crystals of the complexes could not be isolated from any solutions, thus no definite structure could be described. However, the analytical, spectroscopic and magnetic data enable to us propose the possible structures which are shown below in Figure 1-3.

3.7. Radical Scavenging Activity

Radical and reactive oxygen species are related with many diseases such as inflammation, reperfusion injury, atherosclerosis, Alzheimer's disease, and Parkinson's disease etc. So, radical scavenging is very important for antioxidant capabilities of substances. The radical scavenging activity of ligand and its metal complexes were determined by DPPH· and $ABTS^{\bullet+}$ scavenging assays in the present study. DPPH radical scavenging method has been widely used to evaluate the free radical scavenging activity of various antioxidant substances DPPH· concentration changes resulting from the DPPH· reaction with an antioxidant.

During the reaction, DPPH· with an unpaired valence electron at one atom of nitrogen bridge is reduced by a hydrogen atom from an antioxidant (Dawidowicz, et al., 2012).

According to the result of this study, the free radical inhibition of standard antioxidants, ligand and its metal complexes were decreased in the following order: ascorbic acid (95.9%) > BHA (92.7%) > BHT (84.9%) > $[FeL_2]\cdot H_2O$ (54.1%) > $[Zn_2LCl_3(H_2O)_5]\cdot6H_2O$ (49.7%) > L (6.5%) > $[MnLCl(H_2O)_2]\cdot2H_2O$ (3.9%) in presence of same concentration (30 µg/mL) of test sample. So, it was observed that Fe(II) and Zn(II) complexes of ligand scavenged approximately half of DPPH radicals (Figure 4(a)).

ABTS radical cation scavenging assay is another commonly used method to measure radical scavenging activity. According to the result of this study, the ABTS$^{\bullet+}$ radical scavenging activity of standard antioxidants, ligand and its metal complexes were decreased in the following order: ascorbic acid (99.6%) > BHT (99.5%) > BHA (99.1%) > L (98.3%) > $[MnLCl(H_2O)_2]\cdot 2H_2O$ (71.8%) > $[FeL_2]\cdot H_2O$ (32.2%) in presence of same concentration (30 µg/mL) of test sample. Zn(II) complex of ligand did not show significant ABTS$^{\bullet+}$ radical scavenging activity. Especially, only ligand scavenged ABTS$^{\bullet+}$ radicals, effectively (Figure 4(b)).

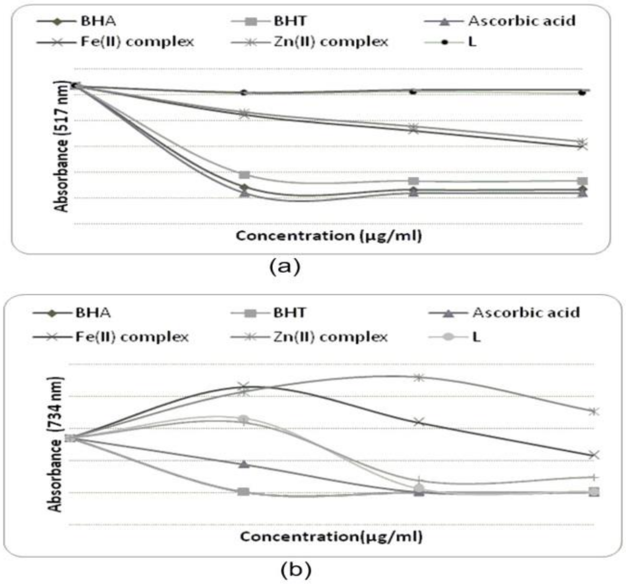

Fig. 4: DPPH$^{\bullet}$ and ABTS$^{\bullet+}$ radical scavenging activity of ligand and its metal complexes (a). DPPH$^{\bullet}$ radical scavenging activity (b). ABTS$^{\bullet+}$ radical scavenging activity

3.8. Ferric Reducing Antioxidant Power (FRAP)

The reduction capacity is an important property of potential antioxidant activity. Antioxidant compounds are able to give electrons or hydrogen atoms to the reactive radicals, reducing them into more stable and unreactive species (Dawidowicz, et al., 2012). Reducing power of ligand and its metal complexes were investigated by FRAP assay. Antioxidant compounds cause the reduction of Fe^{3+}/ferricyanide complex to the ferrous (Fe^{2+}) form because of their reductive capabilities. Reduction can be measured by increasing absorbance at 700 nm. According to this method, higher absorbance indicates a higher ferric reducing antioxidant power.

As shown in Figure 5, reducing power of ligand and its metal complexes were increased like standard antioxidants by increasing concentration. The reducing power of samples and standard antioxidants decreased in the order of BHA > BHT >

Ascorbic acid> L > $[FeL_2]\cdot H_2O$ > $[Zn_2LCl_3(H_2O)_5]\cdot 6H_2O$ > $[MnLCl(H_2O)_2]\cdot 2H_2O$ in presence of 30 µg/mL test sample.

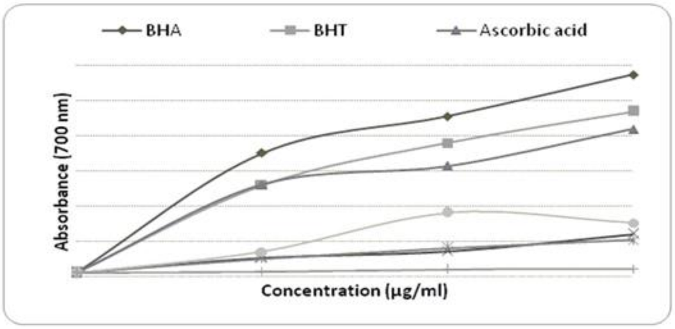

5: Reducing activity of ligand and its metal complexes by FRAP assay

3.9. Total Antioxidant Activity Determination

The ferric thiocyanate method was used to evaluate the effect of ligand and its metal complexes on the prevention of peroxidation of linoleic acid emulsion, as described previously (Dawidowicz, et al., 2012).

The protective effects of samples on lipid peroxidation of linoleic acid emulsion at the same concentration (20 µg/mL) are presented in Figure 6. The percentage of inhibition was calculated at the maximum absorbance point of control (96^{th} hour). The inhibition standard antioxidants, ligand and its metal complexes were decreased in the following order: L (66.6%) > ascorbic acid (63.0%) > BHT (57.5%) > $[Zn_2LCl_3(H_2O)_5]·6H_2O$ (55.6%) > BHA (52.5%) > $[FeL_2]·H_2O$ (37.5%) > $[MnLCl\ (H_2O)_2]·2H_2O$ (32.2%) in presence of same concentration (20 µg/mL) of test sample. These results indicate that ligand had effective antioxidant activity in the ferric thiocyanate assays in Table 1. Similarly, ligand was showed great antioxidant activity by other both methods, FRAP and ABTS assays.

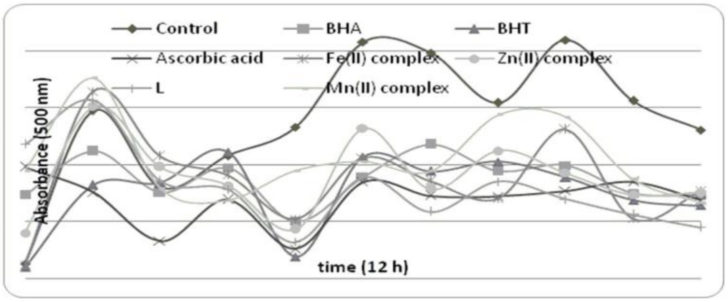

Fig. 6: Total antioxidant activities of ligand and its metal complexes and standard antioxidant compounds by ferric thiocyanate method

Table 1: Percentages of radical scavenging and percentages of inhibition of linoleic acid peroxidation

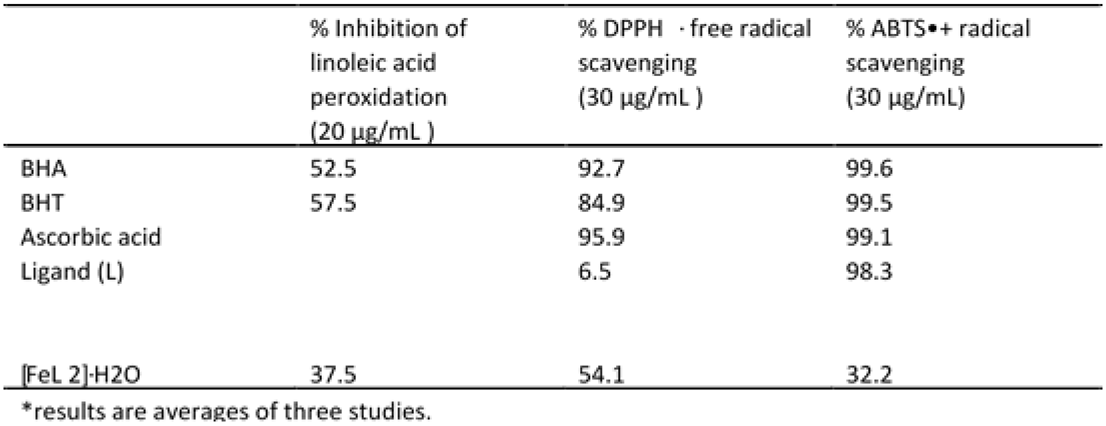

	% Inhibition of linoleic acid peroxidation (20 µg/mL)	% DPPH · free radical scavenging (30 µg/mL)	% ABTS•+ radical scavenging (30 µg/mL)
BHA	52.5	92.7	99.6
BHT	57.5	84.9	99.5
Ascorbic acid		95.9	99.1
Ligand (L)		6.5	98.3
[FeL 2]·H2O	37.5	54.1	32.2

*results are averages of three studies.

66.6 63.0

[Zn2LCl3(H2O)5]·6H2O 55.6 49.7 [MnLCl(H2O)2]·2H2O 32.2 3.9 71.8

4. Conclusion

In this paper, we report the synthesis and characterization of a thiophene-carboxylate ligand derived from ethyl 2-amino-6-methyl-4,5,6,7-tetrahydrobenzo[b]thiophene-3-carboxylate and salicylaldehyde, and its complexes with Zn(II), Fe(II) and Mn(II). In addition to that antioxidant property of ligand and its complexes was examined. The structure of the ligand and its complexes was determined on the basis of elemental analyses, molar conductivities, magnetic susceptibility, IR spectra, UV–Vis., mass spectra, ^{1}H-NMR, ^{13}C-NMR spectra and thermo gravimetric analyses.

All these studies give good evidence for the proposed structure. The results of this study clearly indicate that ligand and its metal(II) complexes have effective and potent antioxidant properties.

5. Conflict of Interest

The authors declare that there is no conflict of interests regarding the publication of this article.

6. Acknowledgements

This study was financially supported by Scientific Research Projects Unit of Muş Alparslan University (project no: FEF0049-0004).

7. References

Ahmed, Riyadh M., Yousif, Enaam I. and Al-Jeboori, Mohamad J. (2013). Co(II) and Cd(II) complexes derived from heterocyclic Schiff-bases: synthesis, structural characterization, and biological activity. The Scientific World Journal, 2013, 6.

Ali, M.A., Fernando, K.R., Palit, D., Nazimuddin, M. (1995). The Preparation and characterization of some new nickel(II), copper(II), zinc(II) and cadmium(II) complexes of the pyrrole-2-carboxaldehyde Schiff bases of S-alkyl esters of dithiocarbazic acid. Transition Met. Chem., 20, 19-22.

Al-Juburi, Ruaa M. (2012). Synthesis and characterization of some heterocyclic compounds (oxazepine, tetrazole) derived from Schiff bases. Journal of AlNahrain University, 15(4), 60-67.

Bursal, E., Gulcin, I. (2011). Polyphenol contents and in vitro antioxidant activities of lyophilized aqueous extract of kiwifruit (*Actinidia deliciosa*). Food Res. Int., 44(5), 1482-1489.

Bursal, E., Koksal, E. (2011). Evaluation of reducing power and radical scavenging activities of water and ethanol extracts from sumac *(Rhus coriaria L*). Food Res. Int., 44(7), 2217-2221.

Dawidowicz, A.L., Wianowska, D., Olszowy, M. (2012). On practical problems in estimation of antioxidant activity of compounds by DPPH method (problems in estimation of antioxidant activity). Food Chem., 131, 1037-1043.

El-Masry, A.H., Fahmy, H.H., Abdelwahed, S.H.A. (2000). Synthesis and antimicrobial activity of some new benzimidazole derivatives. Molecules, 5, 1429-1438.

Etaiw, Safaa Eldin H., Abd El-Aziz, Dina M., Abd El-Zaher, Eman H., Elham A. Ali. (2011). Synthesis, spectral, antimicrobial and antitumor assessment of Schiff base derived from 2-aminobenzothiazole and its transition metal complexes. Spectrochim. Acta Part A, 79, 1331-1337.

Gulcin, I., Bursal, E., Sehitoğlu, H.M., Bilsel, M., Goren, A.C. (2010). Polyphenol contents and antioxidant activity of lyophilized aqueous extract of propolis from Erzurum. Food Chem. Toxicol., 48(8,9), 2227-2238.

Ilhan, S., Baykara, H., Oztomsuk, A., Okumus, V., Levent, A., Seyitoglu, M.S., Ozdemir, S. (2014). Synthesis and characterization of 1,2-bis(2-(5-bromo-2hydroxybenzilidenamino)-4-chlorophenoxy)ethane and its metal complexes: An experimental, theoretical, electrochemical, antioxidant and antibacterial study. Spectrochim. Acta Part A Mol. Biomol. Spectrosc., 118, 632-642.

Jezowska-Trzebiatowska, B., Lisowski, J., Vogt, A., Chmielewski, P. (1988). Synthesis and characterization of Fe(III), Co(II), Ni(II), Cu(II) and Zn(II) complexes with N-salicydene-*o*-hydroxymethyleneaniline. Polyhedron, 7, 337-343.

Jouad, E.M., Riou, A., Allian, M., Khan, M.A., Bouet, G.M. (2001). Synthesis, structural and spectral studies of 5-methyl 2-furaldehyde thiosemicarbazone and its Co, Ni, Cu and Cd complexes. Polyhedron, 20, 67-74.

Kabeer, A.S., Baseer, M.A., Mote, N.A. (2001). Synthesis and antimicrobial activity of some Schiff bases from benzothiazoles. Asian. J. Chem., 13(2), 496-500.

Kiran, S., Manjeet, S.B., Parikshit, T. (2006). Synthesis, characterization and biological studies of Co(II), Ni(II), Cu(II) and Zn(II) complexes with bidentate Schiff bases derived by heterocyclic ketone. Eur. J. Med. Chem., 41, 147-153.

Koksal, E., Gulcin, I., Beyza, S., Sarıkaya, O., Bursal, E. (2009). In vitro antioxidant activity of silymarin. J. Enzym Inhib. Med. Chem., 24(2) 395-405.

Lever, A.B.P. (1984). Inorganic Electronic Spectroscopy. (2nd edn.). Elsevier, Amsterdam.

Manjunatha, M., Naik, V.H., Kulkarni, A.D., Patil, S.A. (2011). DNA cleavage, antimicrobial, antiinflammatory anthelmintic activities, and spectroscopic studies of Co(II), Ni(II), and Cu(II) complexes of biologically potential coumarin Schiff bases. J. Coord. Chem., 64(24), 4264-4275.

Mohamed, G.G. (2001). Metal complexes of antibiotic drugs. Studies on dicluxacillin complexes of Fe-II, Fe-III, Co-II, Ni-II and Cu-II. Spectrochim. Acta Part A, 57(8), 1643-1648.

Moustafa, M.M. (1997). Spectrophotometric analysis, thermal analysis and gravimetric determination of some metal ions with oxime and Schiff's base derivatives of N-furoylphenylhydroxylamine. J. Thermal Anal., 50, 463-471.

Padma Priya, N., Arunachalam, S., Manimaran, A., Muthupriya, D., Jayabalakrishnan, C. (2009). Mononuclear Ru(III) Schiff base complexes synthesis, spectral, redox, catalytic and biological activity studies. Spectrochim. Acta Part A Mol. Biomol. Spectrosc., 72(3), 670-6.

Rabbi, M.F., Finnegan, A., Al-Hartli, L., Stong, S. and Roebuck, K. A. (1998). Interleukin-10 enhances tumor necrosis factor-alpha activation of HIV-1 transcription in latently infected T cells. Journal of Acquired Immune Deficiency Syndromes & Human Retrovirology, 19(4), 321-333.

Ramesh, R., Sivagamasundari, M. (2003), Synthesis, spectral and antifungal activity of Ru(II) mixed-ligand complexes. Syn. React. Inorg. Met. Org. Chem., 33, 899910.

Sharaby, C.M. (2005). Preparation, characterization and biological activity of Fe(III), Fe(II), Co(II), Ni(II), Cu(II), Zn(II), Cd(II) and UO_2(II) complexes of new cyclodiphosph(V)azane of sulfaguanidine. Spectrochim. Acta Part A, 62(1), 326-334.

Yu, T.Z., Zhang, K., Zhao, Y.L., Yang, C.H., Zhang, H., Qian, L., Fan, D.W., Dong, W.K., Chen, L.L., Qiu, Y.Q. (2008). Synthesis, crystal structure and photoluminescent properties of an aromatic bridged Schiff base ligand and its zinc complex. Inorg. Chim. Acta, 361, 233-240.